JOURNAL OF Applied Polymer SCIENCE

Integrated PLGA–Ag Nanocomposite Systems to Control the Degradation Rate and Antibacterial Properties

Silvia Rinaldi,[1*] Elena Fortunati,[2] Marco Taddei,[1] Josè M. Kenny,[2,3] Ilaria Armentano,[2] Loredana Latterini[1]

[1]Dipartimento di Chimica and Centro di Eccellenza sui Materiali Innovativi Nanostrutturati (CEMIN), Università di Perugia Via Elce di Sotto 8, 06123 Perugia, Italy

[2]Centro di Ingegneria dei Materiali, UdR INSTM, NIPLAB, Università di Perugia, Terni, Italy

[3]Institute of Polymer Science and Technology, CSIC, Juan de la Cierva 3, 28006, Madrid, Spain

*Present address: Dipartimento di Chimica, Università di Siena, Via A. De Gasperi, 2 (Quartiere di S. Miniato) 53100 Siena, Italy.
Correspondence to: L. Latterini (E-mail: loredana@unipg.it) or I. Armentano (E-mail: ilaria.armentano@unipg.it.)

ABSTRACT: Biodegradable polymer based nanocomposite materials have attracted much attention since they can be used for biomedical and pharmaceutical applications. In order to have highly integrated PLGA nanocomposite materials, silver colloidal nanoparticles were prepared in chloroform starting from silver nitrate and using polyvinylpyrrolidone as reduction and capping agent. TEM and AFM imaging give information on the size distribution of the silver nucleus (7.0 nm) and the capping shell (8.2–10.7 nm). PLGA–Ag nanocomposites were prepared upon addition of 1 or 3% wt of silver nanoparticles to the PLGA/chloroform suspension. The effect of silver loading on polymer degradation was studied following the mass loss and the morphology of nanocomposite films at different degradation stages. The concentrations of Ag^+, which is released during nanocomposite degradation, were monitored and analyzed through the diffusion model, to have insight on the degradation kinetics. The release rate, and likely the degradation rate, was reduced at higher silver loading. Bacterial growth tests indicated that the cell growth is inhibited in the presence of PLGA–Ag nanocomposites and the efficiency is correlated to Ag^+ release. Thus, controlling the nanoparticle loading, a tunable degradation and antibacterial action can be designed. © 2013 Wiley Periodicals, Inc. J. Appl. Polym. Sci. 130: 1185–1193, 2013

KEYWORDS: nanoparticles; nanowires and nanocrystals; biodegradable; composites; degradation; biomedical applications

Received 4 January 2013; accepted 6 March 2013; Published online 19 April 2013
DOI: 10.1002/app.39255

INTRODUCTION

Poly(DL-Lactic-*co*-Glycolic acid) (PLGA) copolymers have been widely utilized as biomaterials for delivery systems or implanted medical devices;[1–4] however, such devices often cause bacterial infections, which limit their applications.[5] PLGA is a biodegradable polymer since in water media it undergoes hydrolytical chain scission; the mechanism of the degradation occurs in different steps involving water penetration, chain scission and diffusion processes of the degradation products.[1,2,6] It has been proven that the occurrence of the latter processes impacts the polymer degradation rate since the acid products act as catalyst for the next hydrolytic steps. Several factors can affect the degradation rate of PLGA including chemical architecture[7–9] (e.g., molecular weight, length of lactic and glycolic blocks, ratio of lactic and glycolic acids), structure, morphology, and porosity of the polymeric network.[10,11] When the water molecules attack the ester bonds in the polymer chains, the average length of the degraded chains becomes smaller. The process results in short oligomer fragments having carboxylic end groups that render the polymer soluble in water. Very often, the molecular weight of some fragments is still relatively large such that the corresponding diffusion rates are slow. As a result, the remaining oligomers will lower the local pH, catalyze the hydrolysis of other ester bonds and speed up the degradation process. This autocatalytic mechanism is frequently observed in thick biodegradable materials.[10–13]

However, it has been reported that inorganic nanoparticles alter the degradation behavior of PLGA since they can buffer the environment, thus reducing the autocatalytic action of the acidic end groups created by chain scission or affecting the diffusion rates of the acidic products.[14] On the other hand, the dispersion of an inorganic nanofiller phase (as silver nanoparticles) in a organic and hydrophobic polymer can modify the

Additional Supporting Information may be found in the online version of this article

matrix surface and the thermal properties and affect the polymer degradation process.[15–18] The composite degradation behavior can be due to the combination of the filler dispersion and morphological changes induced by the hydrophilic filler.[14]

Over the past decade nanocomposites obtained by dispersion of inorganic nanoparticles in polymeric matrices have attracted great interest, both in industry and in academia, because the presence of nanofillers affords a remarkable improvement of the material properties when compared to those of the virgin polymer or of conventional macro- and micro-composites. The improvements can include mechanical properties, heat resistance, flammability, gas permeability, and biodegradability of biodegradable polymers.[19–23] Moreover, the nanocomposites may show additional specific properties if the fillers are properly designed, i.e. linear and non-linear optical properties or biological activity.[24] Metal nanoparticles have attracted great interest for their unique optical, electrical, catalytic, and biomedical properties.[25–29] In particular, biodegradable nanocomposites based on metal nanoparticles such as gold, titanium, and silver have been applied as sensors or transducers, for the diagnosis and treatment of diseases.[28,29] It has been demonstrated that upon loading PLGA with silver nanoparticles, the bacterial development was strongly reduced, mainly through a modification of the surface properties.[30,31]

However, the chemical nature of the nanoparticles, their capping agent and even the medium where they are prepared might play an important role in determining the interaction between the polymer matrix and the nanofiller thus affecting the dispersion and the bulk behavior of the nanocomposite films.[14,30] Indeed, it has been recently reported that PLGA–Ag nanocomposite films obtained by dispersing water soluble and commercially available silver nanoparticles in PLGA/chloroform suspensions resulted in a surface structuring of the films due to dewetting phenomena.[30,32–34] For many applications, the induced surface roughness might represent a limitation since it can nucleate the formation of precipitates. If surface structuring is not desirable, particular attention has to be paid in the preparation of nanoparticles compatible with the PLGA matrix in order to reduce the occurrence of film rupture and material accumulation during the preparation of nanocomposite films through solvent casting methods.[35,36] The use of inorganic nanoparticles with higher affinity/solubility for the polymer matrix can reduce phase separation processes which occur during polymer dewetting, thus avoiding the film structuring.[37] For this reason, inorganic nanoparticles bearing a polymer stabilizer shell can better disperse in PLGA matrix and reduce the phase separation processes,[38,39] and eventually can affect the polymeric matrix degradation and hence the silver release.

In this study, silver nanoparticles (Ag-NP) stabilized by polyvinylpyrrolidone (PVP) were prepared to be used as nanofiller in PLGA nanocomposite films. The Ag-NP synthesis was designed to control the metal nuclei growth and their dispersion in PLGA matrix was optimized. For these reasons, the Ag-NP were prepared in the same solvent used to solubilize the PLGA pellet (chloroform). The behavior of the PLGA–Ag nanocomposite materials, with different silver loading, has been investigated to obtain information whether Ag-NP affect the polymer degradation mechanism and the antibacterial properties of the nanocomposites during degradation.

EXPERIMENTAL

Materials

$AgNO_3$ (Sigma-Aldrich, ACS reagent, ≥99.0%), polyvinylpyrrolidone (PVP, $M_w = 40$ kDa, Sigma-Aldrich), chloroform ($CHCl_3$, 99.4% GC-grade) were used as received.

Poly(DL-Lactide-*co*-Glycolide) (PLGA) (inherent viscosity, 0.95–1.20 dL/g) ether terminated, an amorphous copolymer with a 50/50 ratio (PLA/PGA), was purchased from Absorbable Polymers-Lactel (Durect Corporation).

Preparation of Silver Colloidal Nanoparticles

$AgNO_3$ (0.0856 g) was added to a PVP/$CHCl_3$ solution (ca. 10% w/v) previously heated to the boiling point. The solution was maintained at this temperature conditions for about 5 h under vigorous stirring to allow nucleation and growth of silver nanoparticles (Ag-NP).

Preparation of Solvent Cast PLGA–Ag Films

PLGA neat films and PLGA–Ag nanocomposites (PLGA/*n*-Ag, where *n* represent the weight percentage of Ag-NP) were produced by the solvent casting technique. Neat PLGA films were obtained dissolving polymer granules in $CHCl_3$ (10% w/v) and using a magnetic stirring at room temperature (RT) to obtain complete polymer dissolution. PLGA nanocomposites were produced adding a certain quantity of PLGA pellets to the pristine or diluted Ag-NP suspensions, in order to maintain the PLGA/$CHCl_3$ at 10% w/v. Thermogravimetric analysis (TGA, Seiko Exstar 6000, Cheshire, UK) with a dynamic scan from 30°C to 600°C at 1°C/min in nitrogen atmosphere was used in order to establish the solid residual of Ag-NP suspensions. Thereafter, the polymer was added to the Ag-NP suspensions, which was then magnetically stirred, until it was completely dissolved. The dispersion was cast in a Teflon® sheet, and the samples were air dried for 24 h, and for a further 48 h in vacuum, at 37°C, allowing the solvent to evaporate. Nanocomposite films 0.3 mm thick, with 1 and 3% wt of Ag-NP with respect to PLGA matrix were produced and designed as PLGA/1-Ag and PLGA/3-Ag, respectively.

Instrumentation

UV–VIS absorption spectra of the Ag-NP suspensions were recorded with a double beam Perkin-Elmer Lambda 800 spectrophotometer.

A Philips mod.208 transmission electron microscope (TEM, operating at 80 kV of beam acceleration) was used to analyze size and size distribution of the nanoparticles. The nanoparticles dissolved in $CHCl_3$/PVP suspensions were deposited in a 400 mesh copper grid coated with formvar. The size distribution histograms were obtained by analyzing 150–200 nanoparticles in each sample.

An atomic force microscope (AFM, Solver-Pro P47H, NT-MDT) was used to record topography and phase images of Ag-NP. The measurements were carried out in semi-contact conditions by use of 190–325 kHz cantilever. A drop of the sample suspended in $CHCl_3$ was placed on a mica substrate and spin coated in order to spread the particles during solvent removal. A grain analysis was carried out to determine the size distribution of the particles from the images. The size distribution

histograms for the samples were obtained by analyzing 150–200 nanoparticles in each sample.

The absorption spectra of the PLGA–Ag samples were recorded by a Varian (Cary 4000, USA) spectrophotometer, which is equipped with a 150 mm integration sphere for reflectance spectra recording. A bar of barium sulfate was used as reference to calibrate the spectrophotometer. The recorded spectra were analyzed with the Kubelka–Munk equation in order to make the comparison among different samples possible.

Thermogravimetric analysis (TGA) was performed using a quartz rod microbalance (Seiko Exstar 6000, Cheshire, UK) on PLGA–Ag systems in order to evaluate the effect of silver nanoparticles on the nanocomposite thermal stability. The measurements were done in the following conditions: 10 mg weight samples, nitrogen flow (250 mL/min), temperature range from 30 to 900°C, 10°C/min heating rate. Thermal degradation temperatures (T_d) were evaluated from TGA thermograms.

Field emission scanning electron microscopy (FESEM, Supra 25-Zeiss, Germany) was used to examine the surface morphology of nanocomposite films and to evaluate the effect of degradation *in vitro* process.

A confocal laser scanning microscope (CLSM, Nikon PCM2000, Italy) was used to investigate the nanocomposite morphology and the nanoparticle dispersion.

The release of metal cation by the nanocomposite materials was monitored by Varian 700-ES series Inductively Coupled Plasma-Optical Emission Spectrometers (ICP-OES) analyzing solutions contacted for different times with the samples. In particular, nanocomposites samples (area 2 cm^2) were incubated in 15 mL of deionized water for up to 15 days to monitor the amount of silver ions released upon polymer degradation; the solutions were stored at 37°C in dark conditions. The solutions were regularly analyzed by ICP to determine the concentration of Ag^+, once the instrumental setup has been calibrated with a standard solution. Experiments were conducted in duplicate.

Degradation Studies

The degradation of the PLGA and PLGA–Ag films was investigated in phosphate buffer saline (PBS) under physiological conditions (pH 7.4 and 37°C). Neat PLGA and nanocomposite samples, at different formulations (PLGA/1-Ag and PLGA/3-Ag) were maintained in PBS for 30 days and the buffer solution was changed once a week. Sample weight, morphological and chemical changes were regularly analyzed during the period of degradation.

Antibacterial Tests

Antibacterial tests were performed by measuring the growth of *Escherichia coli* (*E. coli*) colonies in LB broth medium. *E. coli* was grown overnight in LB medium at 37°C under agitation conditions. After that the washed cells were re-suspended in distilled water to obtain a final bacterial concentration of 10^4 cfu/mL. In order to evaluate the nanocomposite activity against the bacterial colonies and the effects of PLGA degradation, the growth of *E. coli* was monitored in the presence of nanocomposites and neat PLGA films at different degradation stages. Film samples (2 cm^2), previously treated with ethanol (70%) and sterilized water, were exposed to degrading aqueous environments for different times (from 1 to 30 days). At selected exposure times, a known amount of bacterial suspensions (50 μL) was added to the PLGA or nanocomposite systems (1 and 3% wt). Samples were incubated overnight at 37°C under agitation conditions and then the bacterial growth was determined by measuring the samples turbidity (optical density at 600 nm).

All experiments were conducted in duplicate. The degree of antibacterial effect is presented as reduction ratio of bacteria colonies.

RESULTS AND DISCUSSION

Synthesis and Characterization of Silver Nanoparticles

The chemical synthesis of silver nanoparticles (Ag-NP) has been carried out in chloroform, in order to obtain a particles suspension in the same solvent used to dissolve the PLGA pellet. The preparation of Ag-NP in organic solvents was previously reported,[40,41] but in most of the cases, a reducing agent was added or the particle formation was photochemically induced. In this study, silver colloidal nanoparticles are prepared in $CHCl_3$ using $AgNO_3$ and PVP as reactants/reducing agent to minimize the chemical components of the colloidal suspension. PVP was previously used to complex metal cations and assist the particle preparation in organic media[40,41] through hydrothermal or photochemical processes. Thus, the extension of literature hydrothermal methods to low-boiling solvents like $CHCl_3$ is rather challenging, taking into account that the PVP concentration affects the particle size and shape distribution and their stability. This polymer is extremely bio-compatible thus it is suitable for applications in biomedical fields.[42]

To achieve an efficient and controlled particle growth leading to spherical nanostructures (to allow a better analysis of the nanocomposite behavior, see below), the reactant concentrations are optimized; in particular, the PVP concentration is optimized to reach quantitative coordination of Ag^+, an efficient nucleation process and a good stability of silver colloids. The formation of Ag-NP has been monitored by spectrophotometric measurements on the reaction mixtures. The presence of an intense absorption band centered at 422 nm in the extinction spectrum (Figure 1), which was assigned to the Surface Plasmon Resonance band of Ag-NP, in agreement with literature data,[43] confirms the formation of Ag colloids in $CHCl_3$.

TEM imaging has been used to analyze the size and morphology of metal nanostructures. Figure 2(A) shows that the obtained suspensions are characterized by quasi-spherical silver nanoparticles, which do not form aggregates. Diameter distribution histogram [Figure 2(B)] is built from TEM images and analyzed by Gaussian functions. The analysis indicates that the diameter distribution is centered at 7.0 ± 0.2 nm and presented 1.3 ± 0.1 nm as full width at half maximum (FWHM), indicating a good dispersion parameter. AFM imaging [Figure 2(C)] has been used to access size information on the whole particles (metal nucleus and polymer shell) to estimate the dimension of the stabilizer shell. Two particles populations with similar averaged dimensions (23.4 ± 0.5 and 28.3 ± 0.9 nm) but different

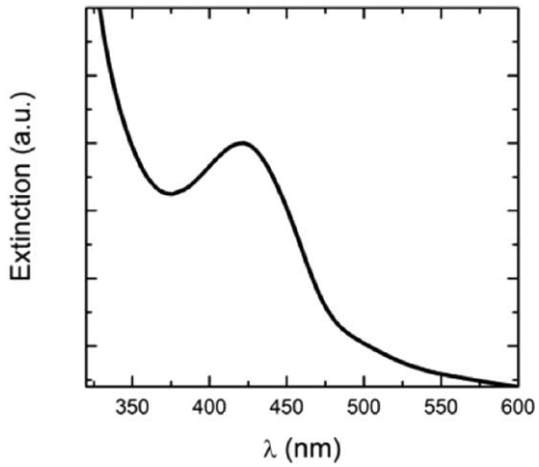

Figure 1. Extinction spectrum of silver colloidal nanoparticles in $CHCl_3$.

FWHM (2.5 ± 0.5 and 19.2 ± 1.8 nm, respectively) were necessary to reproduce the height distribution histograms, determined by AFM imaging [Figure 2(D)]. This quantitative analysis suggests that the stabilizer shell might have different arrangements around the silver nucleus. The comparison between the center dimension from TEM and AFM histograms allows estimating that PVP shell thickness around the particles is in the 8.2–10.7 nm range. This value is in agreement with literature data for similar systems[44] in which a strong capping effect wanted to be achieved to control the particle growth. Taking into account the material density (10.49 and 1.26 g/cm^3 for silver and PVP, respectively) from the dimension information the ratio of mass weights of the metal nanoparticles and PVP is estimated to be about 0.25. This high concentration ratio between the metal nuclei and the stabilizer ensures the full control of the particle growth, which occurred through an isotropic and diffusion controlled process. This controlled dimension and shape distribution of the colloid avoid the presence of singularity points in the nanocomposite materials.

Thermogravimetric analysis of Ag-NP suspension was performed and the silver content in the as prepared chloroform suspension has been estimated to be around 3 mg/mL; this value is then used to prepare nanocomposite with known Ag-content.

PLGA–Ag Nanocomposite Characterization

PLGA–Ag nanocomposite films (about 0.3 mm thick) were successfully prepared by solvent casting. Nanocomposite films with 1% wt (PLGA/1-Ag) and 3% wt (PLGA/3-Ag) of silver loading were prepared and then characterized.

Thermal analysis (TGA) was conducted on neat PLGA and on PLGA–Ag nanocomposites in order to investigate the thermal

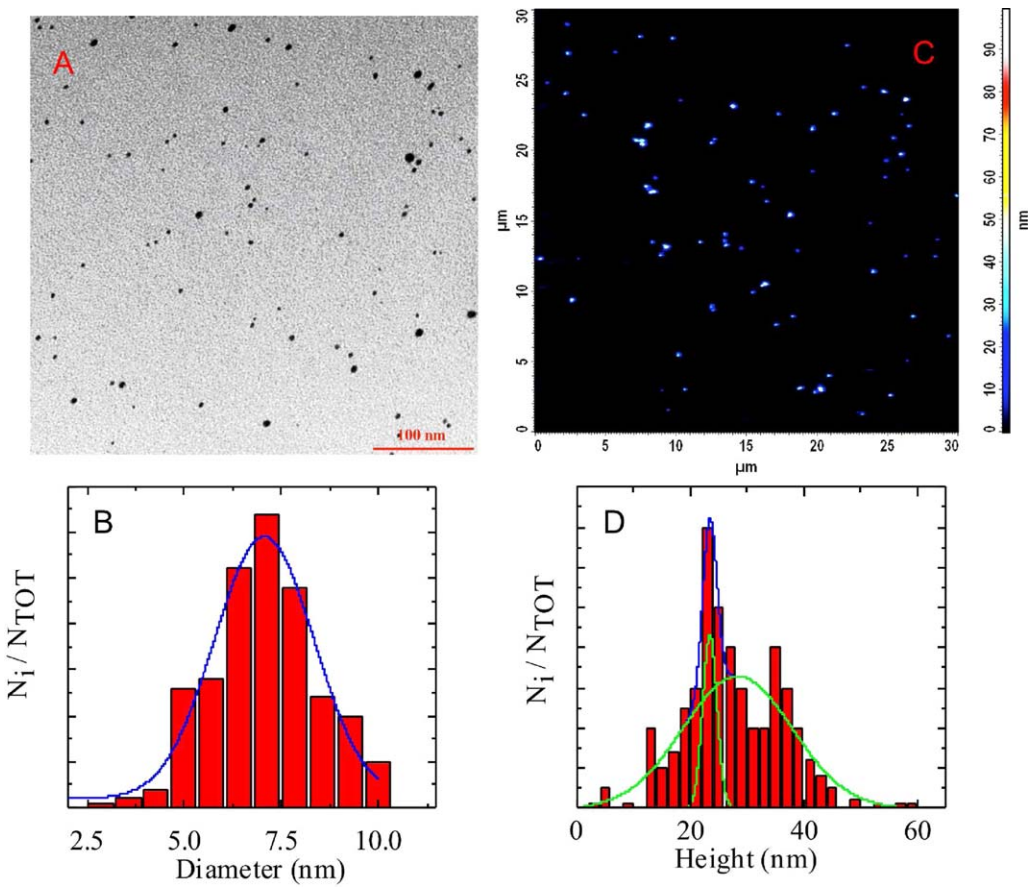

Figure 2. TEM (A, scale bar corresponds to 100 nm) and AFM topography (C, scan area 5×5 μm^2) images of Ag-NP together with size distribution histograms obtained from TEM (B) and AFM (D) images. [Color figure can be viewed in the online issue, which is available at wileyonlinelibrary.com.]

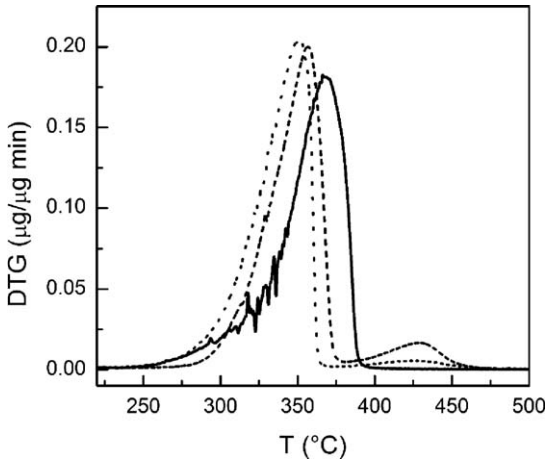

Figure 3. DTG curves of neat PLGA (solid line), PLGA/1-Ag (dotted line), and PLGA/3-Ag (dashed line).

stability of the polymer matrix in the presence of silver nanoparticles. The derivative curves (DTG) of neat PLGA and nanocomposite films (PLGA/1-Ag and PLGA/3-Ag) are shown in Figure 3. PLGA degrades with a single peak at 370°C. A shift to lower degradation temperature (T_d) for PLGA nanocomposites is detected and a T_d of 357°C for PLGA/3-Ag and 350°C for PLGA/1-Ag is observed. In agreement with previous observations,[31] the presence of Ag-NP slightly reduces the thermal stability of the polymer suggesting that in the nanocomposite materials the ordering of the PLGA macromolecules is lower than in neat PLGA; the shape of the DTG profiles indicates that the thermal degradation of PLGA-Ag systems occurs according to the typical PLGA chain scission mechanism. The peak at 420°C, which is present in the PLGA-Ag film thermograms and not visible in the data of PLGA neat system, is associated to the thermal degradation of PVP, which is used as polymeric stabilizer during the nanoparticle synthesis.[45,46]

The presence of metal nanoparticles enhances the thermal conductivity of the nanocomposites, which can speed up the degradation process of the polymeric matrix.[25–27] However, the nanocomposite with 3% wt of silver nanoparticles has shown higher thermal stability respect to PLGA/1-Ag. This behavior can be ascribed to the fact that silver nanoparticles at this concentration (3% wt) affects the motion of polymer chains and they serve as a nucleation site for enhanced nanocomposite crystallization.[47]

Field emission scanning electron microscope images of PLGA/1-Ag and PLGA/3-Ag films are shown in Figure 4. The presence of the silver nanoparticles can influence the viscosity of the system and the evaporation process, resulting in a film structuring.[48–50] The surface of nanocomposites under investigation shows the presence of a faint superficial roughness with some round swelling. However, no regular hole-structures were observed differently from what detected with commercially available hydrophilic silver nanoparticles.[30] In the present samples, PVP acts as a copolymer compatibilizer and assists the dispersion of Ag-NP in the PLGA polymer matrix, so the nanocomposite surface results smooth.

Absorption spectra of PLGA–Ag nanocomposites are reported in Figure 5 and present the SPR band at 430 nm similarly to what observed for the Ag-NP (Figure 1); the UV absorption (in the 270–330 nm region) are likely due to the polymer contributions. The lack of remarkable spectral shift in the SPR band compared to the suspension suggests that the nanoparticles are embedded in the stabilizer shell even in the nanocomposite materials. Furthermore, the band intensity appears proportional to the amount of Ag-NP and no clear spectral broadening due to inter-particle interactions was detected; thus confirming, that PVP acts as compatibilizer in the nanocomposite material.[31] This hypothesis is further supported by the morphological analysis of the samples carried out by using confocal microscopy (Figure 6). The confocal images of the nanocomposite samples were characterized also by a quite homogeneous particle dispersion, differently from what previously observed using surfactant stabilized particles, where solvent assisted structuring was detected.[14,30]

Degradation Behavior of PLGA–Ag Nanocomposites

Figure 7 displays the remaining mass of the degrading PLGA and PLGA–Ag nanocomposite films with different silver nanoparticle content as a function of the incubation time in PBS at 37°C. The dynamics of weight loss for all the nanocomposites are similar to the neat PLGA behavior during hydrolytic degradation process. Initially, for all the studied materials, there is a

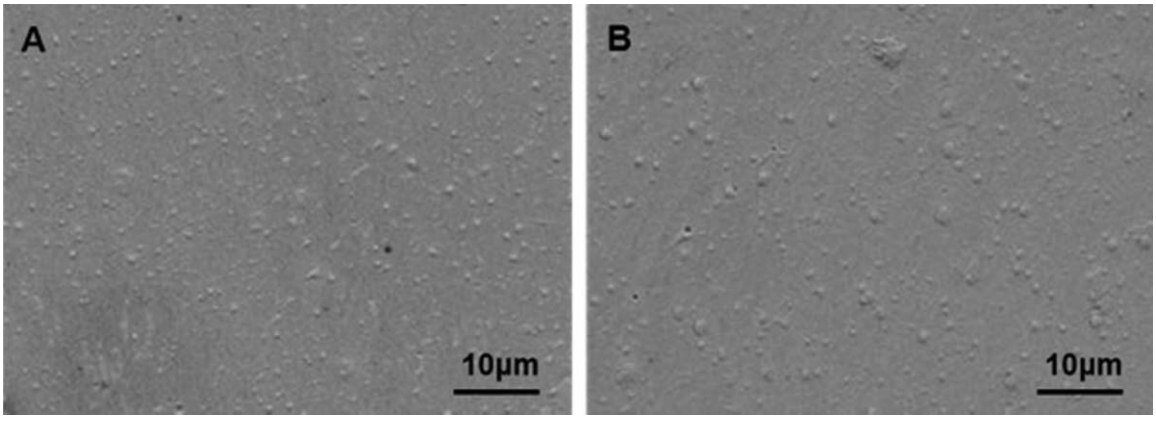

Figure 4. FESEM micrographs of (a) PLGA/1-Ag and (b) PLGA/3-Ag nanocomposite films.

Applied Polymer SCIENCE

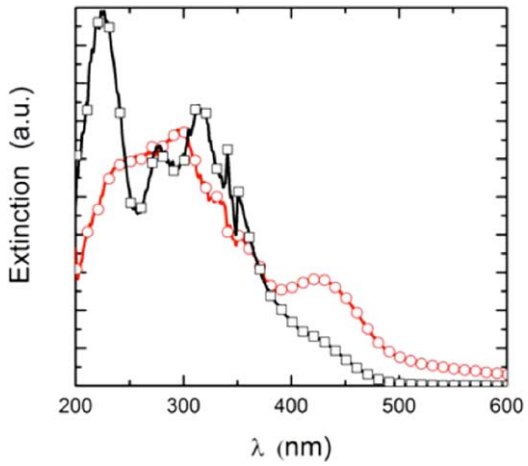

Figure 5. Extinction spectra recorded on PLGA/1-Ag (square) and PLGA/3-Ag (circle) films. [Color figure can be viewed in the online issue, which is available at wileyonlinelibrary.com.]

gradual reduction of the sample mass that continues for several days. The presence of silver nanoparticles slightly affects the weight loss of the polymer matrix, since a higher weight loss is observed for the neat polymer film than for the nanocomposite ones. This observation suggests that the degradation process is slower in the nanocomposite samples.

FT-IR spectra of neat PLGA and PLGA–Ag nanocomposites at different incubation times in aqueous media were recorded (Supporting Information Figure SI1). The data indicate that all the samples present similar features in the FT-IR spectra and also the changes due to degradation were qualitatively similar; thus the samples, despite the Ag-NP content, degrade with the same mechanism. In particular, after 25 days of incubation, in the spectra of PLGA and all nanocomposites the appearance of a broad absorption band centered at 3400 cm^{-1} was observed. This band due to OH stretching,[51] proofs the occurrence of the

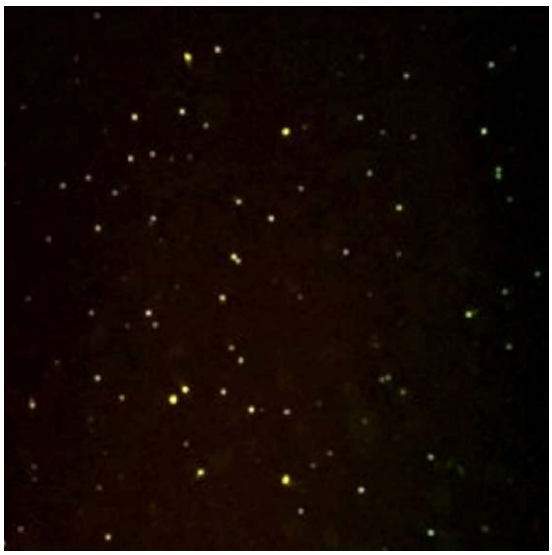

Figure 6. Confocal laser scanning microscopy image recorded on solvent-casted PLGA/3-Ag film (area is 60 × 60 μm^2). [Color figure can be viewed in the online issue, which is available at wileyonlinelibrary.com.]

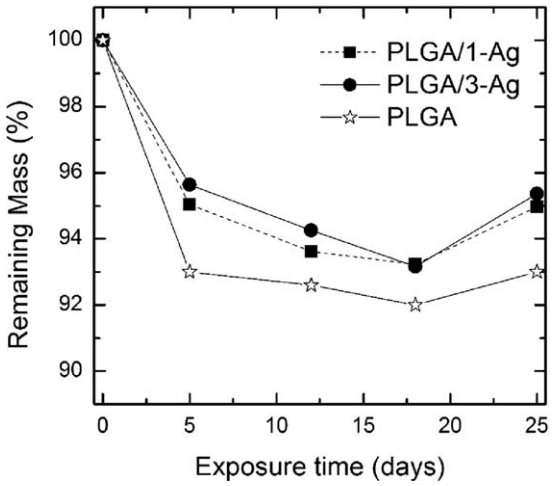

Figure 7. Remaining mass of neat PLGA (star), PLGA/1-Ag (square), and PLGA/3-Ag (circle) as function of exposure time to degrading environment.

hydrolytic process leading to the formation of carboxylic acid end chains which is occurring in the neat PLGA and in the nanocomposites. The carbonyl absorption shows a shift of 4 cm^{-1} during the hydrolytic degradation with a broader peak, and it is visible an important band increase in the frequency region around at 1600 cm^{-1}. Upon sample exposure to the degradation medium, the copolymers characteristic C–O peak at 1168 cm^{-1}, is shifted to the higher frequency and undergoes an intensity change as an effect of the hydrolytic degradation process. Furthermore IR spectra show a preferential reduction of 1422 cm^{-1} band, which corresponds to the asymmetric bending of CH_2 from the glycolic units of the polymer, confirming the preferential degradation of these units, as described in the literature.[52] The remaining polymer is therefore becoming richer in lactic units during degradation.[52]

FESEM images of PLGA neat film and PLGA–Ag nanocomposites recorded before and after different incubation times in PBS at 37°C, allow to evaluate the changes in surface morphology caused by the hydrolysis (Supporting Information Figure SI2). In general, FESEM images show the appearance of superficial defects (holes and cracks) induced by the degradation process whose dimensions and density increased with the time of exposition to the degrading environment. However, the comparison of the images recorded on PLGA and the nanocomposites at the same exposure time suggests that the degree of surface alteration is lower for the nanocomposites than for the neat polymer. Differently from what previously observed,[14] the formation of regular depositions has not been detected in the nanocomposite under investigation.

Once the nanocomposites were exposed to a degrading environment they exhibited a significant enhancement of absorption intensity (Supporting Information Figure SI3). This behavior is likely due to the partial degradation of polymer matrix that leads to a higher exposition of nanoparticulate material on the surface, which can result in the enhancement of cation release. However, the spectrophotometric analysis indicates that no silver nanoparticles, but only silver cations, were released during

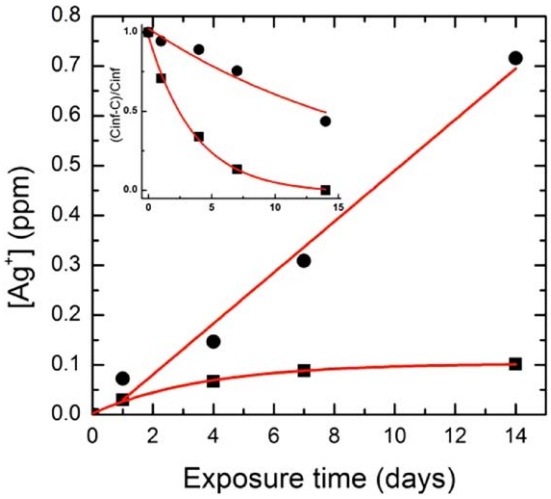

Figure 8. Silver ion release from PLGA/1-Ag (square) and PLGA/3-Ag (circle) during the exposition to the degrading environment; Inset: Release kinetics for the two samples. [Color figure can be viewed in the online issue, which is available at wileyonlinelibrary.com.]

degradation, suggesting that the dispersion of the Ag-NP in the PLGA matrix prevents diffusion and leakage of nanoparticulate matter in the environment reducing the potential hazard of the nanocomposite. However, the full environment-health and safety assessment of the nanocomposite is currently under evaluation.

Silver Ion Release from PLGA–Ag Nanocomposites

The silver ion (Ag^+) release by the nanocomposites with different silver content was monitored during polymer degradation time through periodic analysis by ICP technique. For both the nanocomposite samples, the ion release process started upon exposure to the degrading environment since detectable amounts (about 0.05 ppm) were found already after 24 h of exposition and the amount of Ag^+ increased at longer exposure time along with the polymer degradation (Figure 8). Furthermore, the absolute amount of Ag^+ is dependent on the loading of metallic nanoparticles being higher in the case of PLGA/3-Ag. The analysis of the cation release data through the analytical solution of diffusion model[53] allows determining the kinetic parameters of the release process (Figure 8, inset). In particular, the relative amount of Ag^+ released by the composites has been expressed as $(C_{inf} - C)/C_{inf}$, where C_{inf} is the Ag^+ concentration at infinitive degradation times and C is the Ag^+ measured at defined exposure times, and plotted as function of degradation time (Figure 8, inset). It has to be noted that, for PLGA/1-Ag, the Ag^+ concentration at the plateau (Figure 8) has been considered as C_{inf} value; while for PLGA/3-Ag, the C_{inf} value has been determined by fitting the experimental concentration with a mono-exponential growth function.

The $(C_{inf} - C)/C_{inf}$ data as function of exposure time could satisfactorily be reproduced by mono-exponential functions leading to release lifetime values of 19.3 and 3.7 days for PLGA/3-Ag and PLGA/1-Ag, respectively, thus indicating that the release time is longer for the nanocomposite with higher Ag-NP content. Thus, the release process is associated with the PLGA degradation and the analysis suggests that the polymer degradation is slower in the nanocomposite with higher nanoparticle loading in agreement with mass loss data and FESEM imaging. Since the hydrolytic process occurs with the same mechanism in both nanocomposite materials, as indicated by FT-IR measurements, the observed behavior can be rationalized considering that the particle loading affects the kinetics of degradation. Taking into account that the PLGA degradation occurs through a bulk erosion mechanism[53] and that the degradation process is faster for the neat PLGA than for the nanocomposites (Figure 7), the filler loading either reduce the water diffusion in the polymer matrix or lowered the degradation rate of the polymer backbone. The detection of Ag^+ release already after 24 h of exposure suggests that the nanoparticles reduce the efficiency of the hydrolytic process, likely by inhibiting the catalytic process due to carboxylic acid formation, which occurs during degradation. The inhibition of the acid catalysis can be due to either a buffering influence of the filler or to the enhancement of the products diffusion. At this stage no final mechanism can be drawn, but further experiments are in progress to elucidate this point. However, the present results clearly indicate that the kinetics of the release process can be slowed down with the increase of Ag-NP loading.

Antibacterial Studies

Previous investigations on similar systems[30] revealed that PLGA–Ag nanocomposites display antibacterial activity mainly due to the structure and hydrophobicity of the surface, which reduced the bacterial adherence and growth. The nanocomposites under investigation were designed to minimize the surface structuring; however, the controlled degradation behavior suggests that these materials could find use in medical bandages if antibacterial activity is preserved. The effect of PLGA–Ag nanocomposites on bacterial growth has been investigated at different polymer degradation times. In particular, different PLGA–Ag samples, for both particle loadings, which were preventively exposed to aqueous media were contacted with bacteria suspensions and incubated overnight. The number of colonies that survived to the treatment were then spectrophotometrically determined and compared to cultures contacted with neat PLGA. All the determinations were standardized by control bacterial cultures (which were not contacted with nanocomposites or PLGA).

Figure 9 reports the percentage of bacterial colonies measured after contact with the different samples under investigation as a function of degradation time; the graph shows that the colony growth is inhibited by the polymer degradation corresponding to a closer contact with Ag nanoparticles and/or higher Ag^+ concentration. Moreover, the comparison of the data acquired for the different samples in the same experimental conditions, indicates that antibacterial effects increase with silver loading (Figure 9) since a lower bacterial growth was measured for PLGA/3-Ag nanocomposite.

The results of the bacterial tests clearly demonstrate that the bacterial growth is reduced in the presence of PLGA–Ag nanocomposites under investigation and that the bacteriostatic effect is correlated to the Ag^+ release upon polymer degradation. Thus controlling the Ag-NP dispersion and content, the degradation process and consequently the antibacterial efficiencies

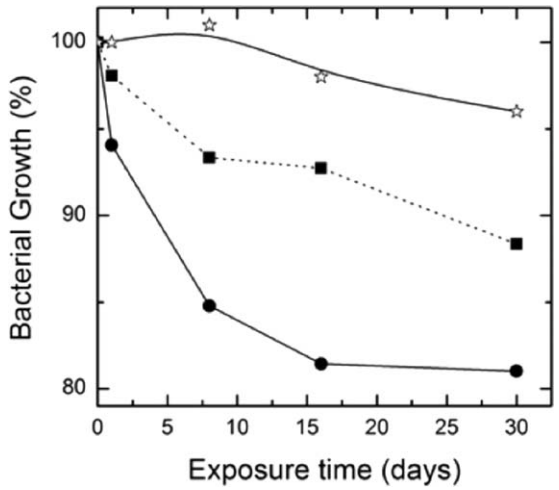

Figure 9. Bacterial growth in the presence of neat PLGA (star), PLGA/1-Ag (square), and PLGA/3-Ag (circle) as function of degradation times.

can be tuned. These observations can definitely help in the design of nanocomposite for bio-medical applications, in which the Ag-NP content can be optimized through chemiometric approaches.

CONCLUSIONS

With the aim to prepare homogeneous PLGA–Ag nanocomposite films with a structureless surface, silver colloidal nanoparticles preparation has been carried out in chloroform to ensure them a good dispersion in PLGA films, which have to be prepared by solvent casting PLGA/$CHCl_3$, suspensions. Silver colloidal nanoparticles are prepared in chloroform by reduction of Ag^+; PVP is used as reduction and capping agent. By optimizing the reactant concentrations, spherical Ag-NP with an average diameter of 7.0 nm are obtained as revealed by TEM and AFM imaging. Nanocomposite films containing silver nanoparticles were prepared by solvent casting process, once different amounts of Ag-NP (1 and 3% wt) have been added to the PLGA/chloroform suspension. FESEM imaging carried out on neat PLGA and nanocomposite films show that in all cases the samples are characterized by structureless surfaces thus confirming that PVP enhanced the Ag-NP dispersion in the PLGA matrix.

The effect of Ag loading on polymer degradation has been investigated following the mass loss and the film morphology at different degradation stages. The data indicate that the metal nanoparticles affect the efficiency of the process but not the mechanism and the degradation temperature. The measurements of silver cation released during polymer degradation indicated that the hydrolytic process and the cation release are coupled. The analysis of the released Ag^+ concentrations, through the diffusion model, enables to obtain the kinetics information on the degradation process. The release time value is longer for the nanocomposite with higher silver loading likely because the Ag-NP reduced in the degradation rate by inhibiting the autocatalytic action.

Bacterial growth tests in the presence of the nanocomposites at different degradation stages indicate that the colony growth is inhibited in the presence of PLGA-Ag nanocomposites and the efficiency is correlated to Ag^+ release. Thus, controlling the Ag-NP loading a tunable antibacterial action can be designed.

The possibility to control PLGA properties by adding specific amount of PVP-stabilized silver nanoparticles represents a key point of material science in different biomedical applications.

ACKNOWLEDGMENTS

Authors thank the Ministero per l'Università e la RicercaScientifica e Tecnologica (Rome) and the National Consortium of Materials Science and Technology (INSTM) for the financial support. Dr. M. Ceccarelli is acknowledged for her assistance in antibacterial tests. E. F. acknowledges L'OREAL Italia for the fellowship "L'Orèal Italia per le Donne e la Scienza 2012" within the project "Progettazione, sviluppo e caratterizzazione di biomateriali nanostrutturati capaci di modulare la risposta e il differenziamento delle cellule staminali".

REFERENCES

1. Ma, P. X. *Mater. Today* **2004**, *7*, 30.
2. Park, G. E.; Pattison, M. A.; Park, K.; Webster, T. *J. Biomaterials* **2005**, *26*, 3075.
3. Sun, B.; Ranganathan, B.; Feng, S. S. *Biomaterials* **2008**, *29*, 475.
4. Wang, Y.; Challa, P.; Epstein, D. L.; Yuan, F. *Biomaterials* **2004**, *25*, 4279.
5. Darouiche, R.O. *Clin. Infect. Dis.* **1999**, *29*, 1371.
6. Kulkarni, A.; Reiche, J.; Lendlein, A. *Surf. Interface Anal.* **2007**, *39*, 740.
7. Cam, D.; Hyon, S. H.; Ikada, Y. *Biomaterials* **1995**, *16*, 833.
8. Heya, T.; Okada, H.; Ogawa, Y.; Toguchi, H. *Int. J. Pharm.* **1991**, *72*, 199.
9. Omelczuk, M. O.; McGinity, J. W. *Pharm. Res.* **1992**, *9*, 26.
10. Fu, B. X.; Hsiao, B. S.; Chen, G.; Zhou, J.; Koyfman, I.; Jamiolkowski D. D.; Dormier, E. *Polymer* **2002**, *43*, 5527.
11. Hurrell, S.; Cameron, R. E. *Biomaterials* **2002**, *23*, 2401.
12. Bikiaris, D. N.; Chrissafis, K.; Paraskevopoulos, K. M.; Triantafyllidis, K. S.; Antonakou, E. V. *Polym. Degrad. Stab.* **2007**, *92*, 525.
13. Yang, Z.; Best, S. M.; Cameron, R. E. *Adv. Mater.* **2009**, *21*, 1900.
14. Fortunati, E.; Latterini, L.; Rinaldi, S.; Kenny, J. M.; Armentano, I. *J. Mater. Sci. Mater. Med.* **2011**, *12*, 2735.
15. Chou, C. W.; Hsu, S. H.; Chang, H.; Tseng, S. M.; Lin, H. R. *Polym. Degrad. Stab.* **2006**, *91*, 1017.
16. Bockstaller, M. R.; Mickiewicz, R. A.; Thomas, E. L. *Adv. Mater.* **2005**, *17*, 1331.
17. Tjong, S. C. *Mater. Sci. Eng. R.* **2006**, *53*, 73.
18. Mai, Y.-W.; Yu, Z.-Z.,Eds. Polymer Nanocomposite; Woodhead-CRC Press: Cambridge, **2006**.
19. Aloisi, G. G.; Costantino, U.; Latterini, L.; Nocchetti, M.; Camino, G.; Frache, A. *J. Phys. Chem. Solids* **2006**, *67*, 909.

20. Aloisi, G. G.; Elisei, F.; Nocchetti, M.; Camino, G.; Frache, A.; Costantino, U.; Latterini, L. *Mater. Chem. Phys.* **2010**, *123*, 372.
21. Latterini, L.; Nocchetti, M.; Costantino, U.; Aloisi, G. G.; Elisei, F. *Inorg. Chim. Acta* **2007**, *360*, 728.
22. Latterini, L.; Nocchetti, M.; Aloisi, G. G.; Costantino, U.; De Schryver, F.; Elisei, F. *Langmuir* **2007**, *23*, 12337.
23. Ricci, M.; Schoubben, A.; Rossi, A.; Blasi, P.; Latterini, L.; Aloisi, G. G.; Rossi, C.; Perioli, L., *Int. J. Pharm.* **2005**, *295*, 47.
24. Lee, J. Y.; Nagahata, J. L. R.; Horiuchi, S. *Polymer* **2006**, *47*, 7970.
25. Latterini, L.; Tarpani, L. *J. Phys. Chem. C* **2011**, *115*, 21098.
26. Gautam, A.; Ram, S. *Mater. Chem. Phys.* **2010**, *119*, 266.
27. Storti, B.; Elisei, F.; Abbruzzetti, S.; Viappiani, C.; Latterini, L. *J. Phys. Chem. C* **2009**, *113*, 7516.
28. Eghlidi, J. F.; Liu, X. Y.; Luan, B.; *J. Mater. Process. Tech.* **2008**, *197*, 428.
29. Ren, J.; Hong, H.; Ren, T.; Teng, T. *React. Funct. Polym.* **2006**, *66*, 944.
30. Armentano, I.; Fortunati, E.; Latterini, L.; Rinaldi, S.; Saino, E.; Visai, L.; Elisei, F.; Kenny, J. M. *J. Nanostruc. Polym. Nanocomp.* **2010**, *6*, 110.
31. An, Y. H.; Friedman, R. J. *J. Biomed. Mater. Res.* **1998**, *43*, 338.
32. Xue, L.; Han, Y. *Prog. Polym. Sci.* **2011**, *36*, 269.
33. Gupta, S.; Zhang, Q.; Emrick, T.; Balazs A. C.; Russel, T. P. *Nat. Mater.* **2006**, *5*, 229.
34. Mukherjee, R.; Das, S.; Das, A.; Sharma, S. K.; Raychaudhuri, A. K.; Sharma, A. *ACS Nano* **2010**, *4*, 3709.
35. Kanemoto, R.; Anas, A.; Matsumoto, Y.; Ueji, R.; Itoh, T.; Baba, Y.; Nakanishi, S.; Ishikawa, M.; Biju, V. *J. Phys. Chem. C* **2008**, *112*, 8184.
36. AbulKashem, M. M.; Perlich, J.; Schulz, L.; Roth, S. V.; Müller-Buschbaum, P. *Macromolecules* **2008**, *41*, 2186.
37. Palza, H.; Vergara, R.; Zapata, P. *Macromol. Mater. Eng.* **2010**, *295*, 899.
38. Luab, Y.; Chen, W. *Chem. Soc. Rev.* **2012**, *41*, 3594.
39. He, R.; Quian, X.; Yin, J.; Zhu, Z. *J. Mater. Chem.* **2002**, *12*, 3783.
40. Butruk, B.; Trzaskowski, M.; Ciach, T. *Mater. Sci. Eng. C* **2012**, *32*, 1601.
41. Bernal, A.; Kuritka, I.; Saha, P. *J. Appl. Polym. Sci.* **2012**, doi:10.1002/app.37723.
42. Curry, A.; Nusz, G.; Chilkoti, A.; Wax, A. *Optic Exp.* **2005**, *13*, 2668.
43. Corbierre, M. K.; Cameron, N. S.; Sutton, M.; Laaziri, K.; Lennox, R. B. *Langmuir* **2005**, *21*, 6063.
44. Kang, J. S.; Kim, K. Y.; Lee, Y. M. *J. Membr. Sci.* **2003**, *214*, 311.
45. Hsu, S.; Chou, S. W.; Tseng, S. M. *Macromol. Mater. Eng.*, **2004**, *289*, 1096.
46. Chou, C.-W.; Hsu, S.-H.; Chang, H.; Tseng, S.-M.; Lin, H.-R. *Polym. Degrad. Stab.* **2006**, *91*, 1017.
47. Buschle-Diller, G.; Cooper, J.; Xie, Z.; Wu, Y.; Waldrup, J.; Ren, X., *Cellulose* **2007**, *14*, 553.
48. Mercado, A. L.; Allmond, C. E.; Hoekstra, J. G.; Filtz-Gerald, J. M. *Appl. Phys. A: Mater. Sci. Process.* **2005**, *81*, 591.
49. Chung, C. W.; Kim, Y. B.; Rhee, Y. H. *Int. J. Biol. Macromol.* **2005**, *37*, 221.
50. Huang, M. H.; Li, S.; Vert, M. *Polymer* **2004**, *45*, 8675.
51. Vey, E.; Roger, C.; Meehan, L.; Booth, J.; Claybourn, M.; Miller, A. F.; Saiani, A. *Polym. Degrad. Stab.* **2008**, *93*, 1869.
52. Charlier, A.; Leclerc, B.; Couarraze, G. *Int. J. Pharm.* **2000**, *200*, 115.
53. von Burkersroda, F.; Scheld, L.; Göpferich, A. *Biomaterials* **2002**, *23*, 4221.